Short Communication

Acetylene Black Loaded on Graphene as a Cathode Material for Boosting the Discharging Performance of Li/SOCl₂ Battery

Jun-Hua Wei[1,3], Xiao-Tian Gao[1], Si-Ping Tan[3], Fang Wang[4], Xiao-Dong Zhu[2,1,*], Ge-Ping Yin[1,*]

[1] School of Chemistry and Chemical Engineering, Harbin Institute of Technology, Harbin 150001, China
[2] Academy of Fundamental and Interdisciplinary Sciences, Harbin Institute of Technology, Harbin 150080, China
[3] Guizhou Meiling battery Co.,Ltd., Zunyi 563003, China
[4] Chemistry and Chemical Engineering Department, College of Life, Tarim University, Alar, 843300, China
[*]Email: zxd9863@163.com, yingphit@hit.edu.cn.

Lithium thionyl chloride (Li/SOCl₂) battery is a promising primary battery owing to its highest theoretical working voltage (3.6 V), excellent output specific energy (up to 590 Wh/kg) and large working temperature interval. However, drawbacks such as insoluble product (LiCl) and non-fully dissolved sulfur deposited on the electrode will cause the failure of the full battery. Herein, we report a cathode material that can boost the discharging performance of Li/SOCl₂ battery by facile assembly of acetylene black nanoparticles on graphene nanosheets. The resulting acetylene black/graphene hybrid exhibits an excellent discharging performance, delivering a capacity as high as 1706 mAh/g at a current density of 5 mA/cm^2.

1. INTRODUCTION

Lithium thionyl chloride (Li/SOCl₂) battery has the highest working potential (3.6 V) and largest actual output specific energy (up to 590 Wh/kg) of all commercial batteries. Moreover, this kind of primary battery can even work at below –80 °C [1,2]. Owing to these merits, Li/SOCl₂ battery is now being widely used in deep space exploration and low-temperature regions. In principle, Li/SOCl₂ battery consists of a lithium anode, a carbon cathode and a non-aqueous SOCl₂/LiAlCl₄

electrolyte in which $LiAlCl_4$ works as both an electrolyte and a cathode active material. The cathode material of compressed carbon black provides a workplace for the reaction between Li and $SOCl_2$ [3]. The reaction can be described as:

$$4Li + 2SOCl_2 \rightarrow 4LiCl\downarrow + S\downarrow + SO_2\uparrow$$
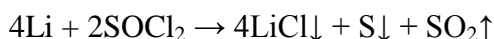
Note that most of sulfur and sulfur dioxide produced during the reaction are dissolved in the excess electrolyte. However, a small amount of released SO_2 may bring stress to the electrode. At the same time, the insoluble product LiCl and non-fully dissolved sulfur may be deposited on the electrode to block the channels [4]. These drawbacks not only lead to the volume expansion, but also hinder the diffusion of the electrolyte and thus cause the concentration polarization and serious heating problems, which may bring about the risk of thermal runaway to $Li/SOCl_2$ battery.

Conventional $Li/SOCl_2$ battery typically uses spherical acetylene black as the cathode material, which the relatively low thermal and electrical conductivity cannot satisfy the requests for high current discharging performance and security [5]. Among other conductive materials, graphene with a unique two-dimensional structure possesses the highest electrical conductivity (10^5–10^6 S/cm) [6], highest thermal conductivity (5800 W/MK) [7] and excellent mechanical flexibility [8]. Once graphene is used as the cathode material of $Li/SOCl_2$ battery, it has the following merits: (1) The exceptionally high electrical conductivity of graphene can significantly reduce the internal resistance and battery heating. (2) The high thermal conductivity can quickly transfer heat, and effectively reduce the risk of thermal runaway. (3) The incredible strength and elasticity can accommodate the volume expansion caused by the deposition of sulfur and the overflow of SO_2, and prevent the structural failure of the full battery.

However, the huge surface area of graphene leads to strong inclination to restack [9,10], which has a negative effect on improving the electrochemical performance of $Li/SOCl_2$ battery. Meanwhile, high preparation cost of graphene restricts its extensive application in $Li/SOCl_2$ battery. Herein, we report a new kind of hybrid cathode material by facile assembly of acetylene black nanoparticles on graphene nanosheets in water. The acetylene black nanoparticles are distributed on the graphene nanosheets at a high concentration and form a micelle-like suprastructure. On the one hand, the graphene nanosheets not only provide excellent mechanical performance and high electrical conductivity, but also prevent the aggregation of the acetylene black nanoparticles. On the other hand, the presence of the acetylene black nanoparticles can effectively isolate the graphene nanosheets from restacking and reduce the quantity of the graphene nanosheets to reduce the cost. Thus, the micelle-like suprastructure can offer more active sites and the higher electrical conductivity to improve the discharging performance and buffer the volume expansion during the discharging process.

2. EXPERIMENTAL

2.1 Oxygen plasma treatment

To enhance the hydrophilicity of the acetylene black nanoparticles and graphene nanosheets, oxygen plasma operated at 100 W was performed. Briefly, 1 g of acetylene black nanoparticles and graphene nanosheets were weighed and loaded in watch glass separately. A constant flow of oxygen

was pumped through the sample space, and the gas was excited by microwave. The samples were exposed in the oxygen plasma for 10 min, and were then collected for further experiments.

2.2 Assembly of acetylene black nanoparticles on graphene nanosheets

Both acetylene black nanoparticles and graphene nanosheets were suspended in deionized water by ultrasonic dispersion at a concentration of 1 mg/mL, and mixed at a volume ratio of 9:1. The mixture was left under strong agitation for 6 h, during which the acetylene black nanoparticles spontaneously adhered to the naked surface of the graphene nanosheets based on van der Waals interaction. The obtained acetylene black/graphene hybrid was collected by vacuum filtration and vacuum-dried at 40 °C overnight.

2.3 Ball-mixing of acetylene black nanoparticles and graphene nanosheets

Acetylene black and graphene were mixed with weight ratios of 9:1. Then the mixture was transformed into a ZrO_2 vessel at a speed of 500 rpm for 2 h.

2.4 Electrochemical tests

A cathode was prepared by mixing 1 g of acetylene black/graphene hybrid, 6 mL of alcohol, 1.5 mL of deionized water and 50 mg of polytetrafluoroethylene emulsion. The obtained slurry was coated on nickel foam. A prismatic cell (ER382575) was equipped in a drying room using Li-B alloy as the anode and 1.8 mol/L of $LiAlCl_4/SOCl_2$ as the electrolyte. The charging test was conducted within a voltage window of 3.7–3.0 V in a BTS battery testing system (Neware, Shenzhen, China). The electrochemical impedance spectroscopy (EIS) test was conducted in a Parstat 2273 advanced electrochemical system within a frequency range from 100 kHz to 100 mHz with the a.c. signal amplitude of 5 mV.

2.5 Characterizations

Scanning electron microscopy (SEM) was performed by a Hitachi SU8010 microscope. X-ray diffraction (XRD) was performed by a PANalytical X'Pert PRO X-ray diffractometer with Cu Kα radiation (λ = 0.154 nm). Brunner–Emmet–Teller (BET) measurement was performed by an ASAP 2020 (Micromeritics).

3. RESULTS AND DISCUSSION

Scheme 1 gives us an overall concept for facile and elegant self-assembly of acetylene black particles on graphene sheets through van der Waals interactions. The oxygen plasma treated acetylene

black and graphene were dispersed in deionized water respectively, then the dispersion liquid was mixed and suffered the sonic treatment process, during which the acetylene black particles were assembly on the graphene sheets.
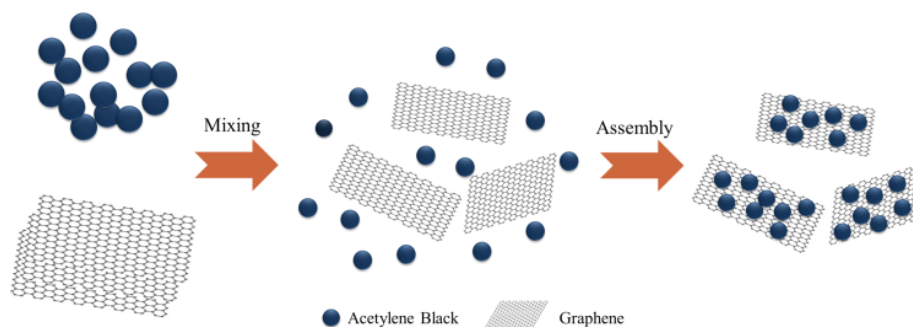
Scheme 1. Schematic illustration of the overall process for the self-assembly of acetylene black particles on graphene sheets through van der Waals interactions.

The morphology of the as-prepared acetylene black/graphene hybrid is characterized by SEM. As shown in Fig. 1a, the commercial acetylene black nanoparticles are homogeneous, and have a spherical morphology with diameters of 50–80 nm. Fig. 1b shows the corrugated morphology of the graphene nanosheets, which are endowed with high elasticity and flexibility character and thought to be important to accommodate the volume expansion during the discharging. Note that for the graphene nanosheets, the huge surface area leads to strong inclination to restack. As such, the acetylene black nanoparticles are attracted to the naked surface of the graphene nanosheets based on van der Waals interaction once they are introduced to stabilize the latter in solvents. In a series of works, Liu and Zhu *et al* have systematically studied the assembly of small entities on various two-dimensional matrices including graphene [11–14], transition metal dichalcogenides [15,16], transition metal oxides [17–19], and *h*-BN [20] in organic solvents based on van der Waals interaction. In this case, interestingly, we find that in deionized water, the oxygen plasma treated acetylene black nanoparticles can also be successfully assembled on the graphene nanosheets, as shown in Fig. 1c. The reason is that after oxygen plasma treatment the acetylene black changed to be hydrophilic and can be well dispersed in deionized water. So it can be attracted to the naked surface of the graphene nanosheets based on van der Waals interaction when they are introduced in solvents. Once being assembled, the acetylene black nanoparticles can effectively reduce the huge surface energy of the graphene nanosheets, thus forming interesting micelle-like suprastructures to stabilize them in deionized water. Compared with the mixture produced by mechanical mixing of the two as shown in Fig. 1d, the acetylene black nanoparticles can be in large quantities and uniformly loaded on the graphene nanosheets by this assembly method.

Fig. 2 shows the XRD patterns of the acetylene black nanoparticles, graphene nanosheets and acetylene black/graphene hybrid, respectively. The sharp peak at 26° correspond to the (002) plane of carbon which shows the unbroken atomic arrangement [21]. It can be informed that there are no

chemical structure changes after the assembly process, so we can easily use the existing materials to design and construct the hybrid materials by this assembly method. This result shows a fantastic potential of this strategy.
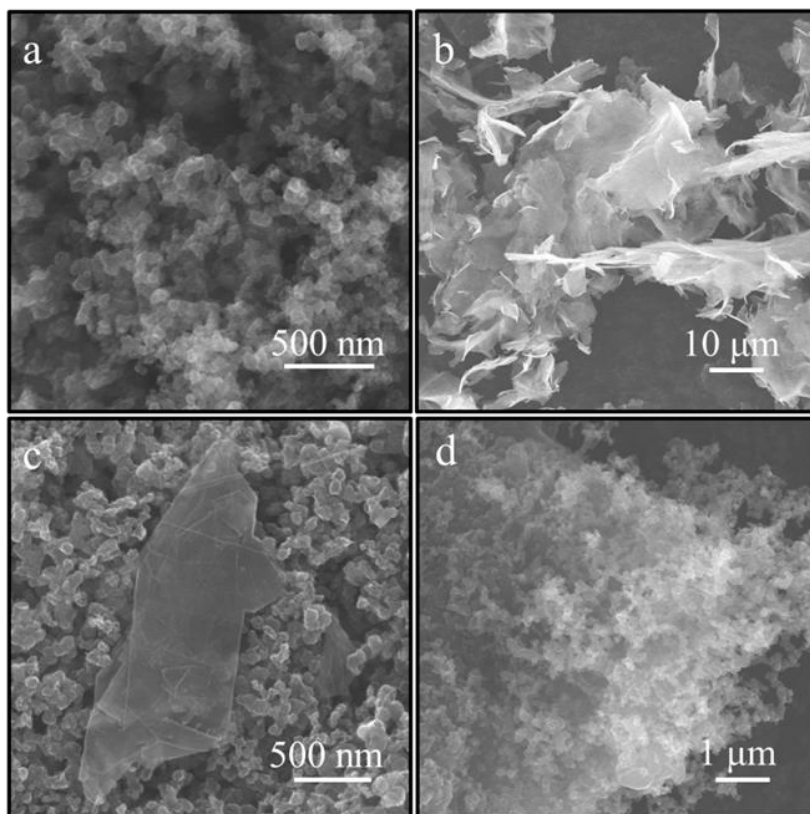

Figure 1. SEM image of a. acetylene, b. graphene sheets, c. acetylene/graphene hybrids produced by mechanical mixing and d. acetylene/graphene hybrids produced by assembly method.
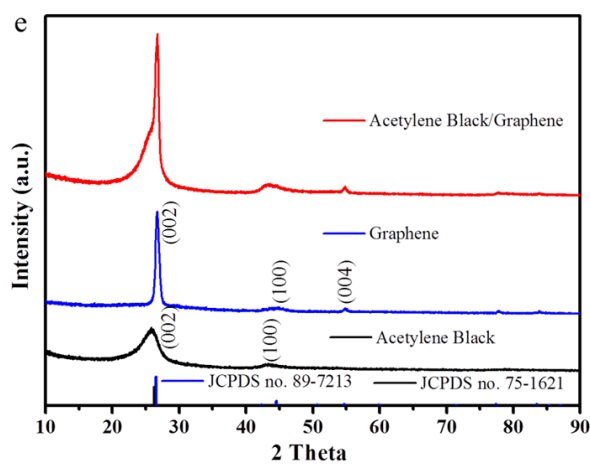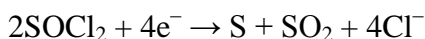

Figure 2. XRD patterns of acetylene black nanoparticles, graphene nanosheets and acetylene black/graphene hybrid.

The discharging performance of the acetylene black/graphene hybrid is tested at a current density of 5 mA/cm^2. The involved electrochemical reaction within the voltage window of 3.7–3.0 V can be described as:

$$2SOCl_2 + 4e^- \rightarrow S + SO_2 + 4Cl^-$$

Insoluble product LiCl and non-fully dissolved sulfur will deposit on the electrode and gradually block the channels which may cause the volume expansion of the cathode. On the other hand, the ion diffusion is hampered, and the concentration polarization increases as a result. These negative effects lead to the failure of the battery. In Fig. 3a, it can be seen that at a current density of 5 mA/cm^2, a steady voltage of 3.464 V can be obtained which is 103 mV higher than that of the mechanical mixture. Moreover, the specific capacity of the acetylene black/graphene hybrid can reach 1706 mAh/g, which is an increase of 13% compared with 1482 mAh/g of the mechanical mixture. Also, this value over those reported previously various cathode materials e.g., AB/NG (1690 mAh/g), Co-N-G (1563 mAh/g), Activated Carbon (887.6 mAh/g), AB/KB (1167 mAh/g), Porous Carbon (710 mAh/g) or Carbon Slurry (1640 mAh/g), as shown in Table 1. This excellent discharging performance is mainly a result of the micelle-like suprastructures obtained during the assembly process.
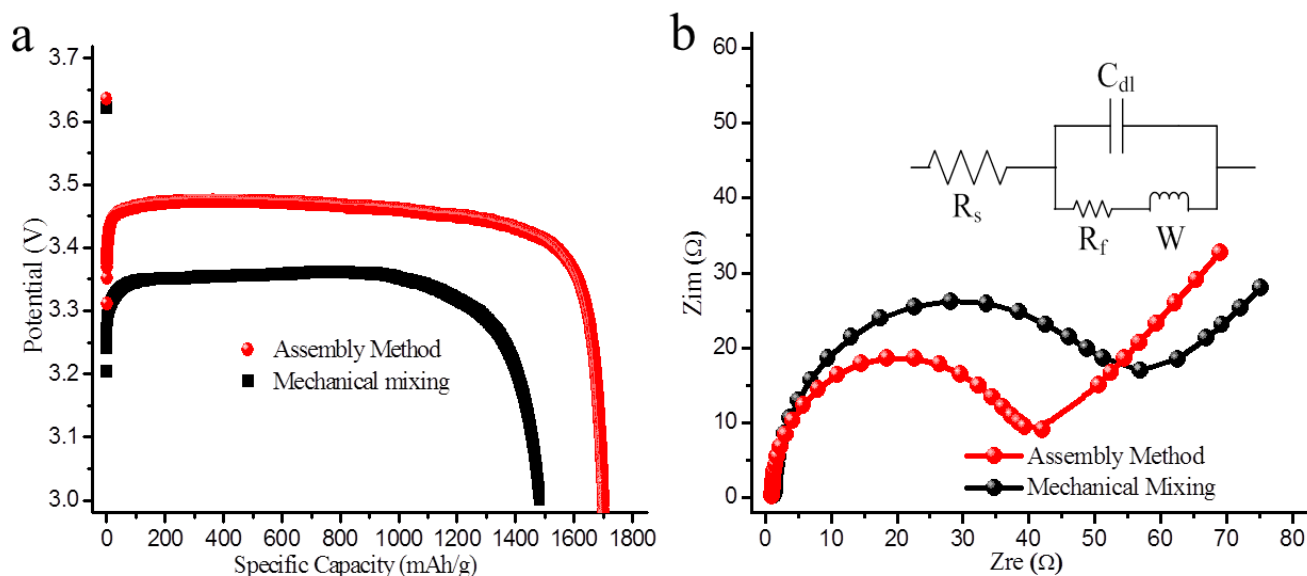

Figure 3. Discharging behaviors and Nyquist plots of acetylene black/graphene hybrid produced by assembly method and acetylene black/graphene mixture produced by mechanical mixing.

To further get clear of the mechanism for the excellent discharging performance of the acetylene black/graphene hybrid, we compare its Nyquist plot with that of the mechanical mixture in Fig. 3b. Both plots have a semicircle at the high–medium frequency and an inclined line at the low frequency, corresponding to charge transfer and solid-state diffusion of lithium, respectively. The inset shows the equivalent circuit. Apparently, the charge transfer resistance of the hybrid is much lower than that of the mechanical mixture (42 *vs.* 55 Ω), proving better electrical conductivity and more

active sites of the former. During the discharging process, the produced LiCl and sulfur will deposit in the channels of the electrode, which may cause the volume expansion of the electrode. On the other hand, the channel blockage increases the concentration polarization, making the battery fail gradually. For the acetylene black/graphene hybrid, the micelle-like suprastructures offer more active sites, which can weaken the negative effect caused by the channel blockage. Moreover, the flexible structure of the acetylene black/graphene hybrid can buffer the volume expansion during the discharging process. Therefore, the specific capacity and security of the acetylene black/graphene hybrid can be improved significantly.

Table 1. Comparison among different Carbon-based cathode materials of Li/SOCl$_2$ battery

Material	Current Density （mA/cm^2）	Capacity （mAh/g）	Reference
AB/G (Assembly Method)	5	1706	This Work
AB/G (Mechanical Mixing)	5	1482	This Work
AB/NG	25	1690	Reference 22.
Co-N-G	25	1563	Reference 23.
Activated Carbon	10	887.6	Reference 24.
AB/KB	50	1167	Reference 25.
Porous Carbon	20	710	Reference 26.
Carbon Slurry	50	1640	Reference 27.

AB: Acetylene Black KB: Ketjen Black G: Graphene NG: N-doped Graphene

4. CONCLUSION

In conclusion, we report a simple route to developing an excellent cathode material by facile assembly of acetylene black nanoparticles on graphene nanosheets. The acetylene black nanoparticles are distributed on the graphene nanosheets at a high concentration, and form a micelle-like suprastructure. On the one hand, the graphene nanosheets not only provide excellent mechanical performance and high electrical conductivity, but also prevent the aggregation of the acetylene black nanoparticles. On the other hand, the presence of the acetylene black can effectively isolate the graphene nanosheets from restacking and reduce the quantity of the graphene nanosheets to reduce the cost. Moreover, the micelle-like suprastructure can offer more active sites to suppress the electrode blockage caused by to the deposition of LiCl and sulfur. The resulting acetylene black/graphene hybrid exhibits an excellent discharging performance, delivering a specific capacity as high as 1706 mAh/g at a current density of 5 mA/cm^2.

References

1. J. L. Li, C. Daniel and D. Wood, *J. Power Sources.*, 196 (2011) 2452.
2. W.C. West, A, Shevade and J, Soler, *J. Electrochem. Soc.*, 157 (2010) 571.
3. S.-B. Lee, S.-I. Pyun and E,-J, Lee, *Electrochim. Acta.*, 47 (2001) 855.
4. Z. Zhang, L. Kong, Y. Xiong, Y. Luo and J. Li, *J. Solid State Electrochem.*, 18 (2014) 3471.
5. R. Zhang, R. Wan, K. Luo, W. Zhang, J. Zhao and S. Zhang, *J. Electrochem. Soc.*, 161(2014) 941.
6. J.-L. Cheng, B. Wang, H.-L. Xin, G.-C. Yang, H.-Q. Cai and F. H. Huang, *J. Mater. Chem. A*, 1(2013) 10814.
7. M.-T. Pettes, I. Jo, Z. Yao and L. Shi, *Nano Lett.*, 11 (2011) 1195.
8. U. Stöberl, U. Wurstbauer, W. Wegscheider, D. Weiss and J. Eroms. *Appl. Phys. Lett.*, 93 (2008) 051906.
9. K. Liu, L. Liu, Y. Luo and D. Jia, *J. Mater. Chem.*, 22 (2012) 20342.
10. P. Martin, *Chem. Soc. Rev.*, 39 (2010) 46.
11. L. Pan, X.-D. Zhu, X.-M. Xie and Y.-T. Liu, *Adv. Funct. Mater.*, 25 (2015) 3341.
12. L. Pan, Y. Liu, X. Xie, X. Ye and X. Zhu, *Nano Res.*, 9 (2016) 2057.
13. X.-T. Gao, X.-D. Zhu, S.-R. Le, D.-J. Yan, C.-Y. Qu, Y.-J. Feng, K.-N. Sun and Y.-T. Liu, *ChemElectroChem*, 2016, DOI: 10.1002/celc.201600305.
14. L. Pan, X.-D. Zhu, K.-N. Sun, Y.-T. Liu, X.-M. Xie and X.-Y. Ye. *Nano Energy*, 30 (2016) 347.
15. L. Pan, X.-D. Zhu, X.-M. Xie and Y.-T. Liu, *J. Mater. Chem. A*, 3 (2015) 2726.
16. X.-D. Zhu, K.-X. Wang, D.-J. Yan, S.-R. Le, R.-J. Ma, K.-N. Sun and Y.-T. Liu, *Chem. Commun.*, 51 (2015) 11888.
17. L. Pan, K.-X. Wang, X.-D. Zhu, X.-M. Xie and Y.-T. Liu, *J. Mater. Chem. A*, 3 (2015) 6477.
18. H. Xu, X.-D. Zhu, K.-N. Sun, Y.-T. Liu and X.-M. Xie, *Adv. Mater. Interfaces*, 2 (2015) 1500239.
19. D.-J. Yan, X.-D. Zhu, K.-X. Wang, X.-T. Gao, Y.-J. Feng, K.-N. Sun and Y.-T. Liu, *J. Mater. Chem. A,* 4 (2016) 4900.
20. Z.-Q. Duan, Y.-T. Liu, X.-M. Xie, X.-Y. Ye and X.-D. Zhu, *Chem. Asian J.*, 11 (2016) 828.
21. Z. Lei, L. Lu and X.-S. Zhao, *Energy Environ. Sci.*, 5 (2012) 6391.
22. B. Li, Z. Yuan, Y. Xu and J. Liu, *Appl. Catal. A: Gen.*, 523 (2016) 241.
23. B. Li, Z. Yuan, Y. Xu and J. Liu, *Electrochim. Acta*, 217 (2016) 73.
24. S. Wang, J. Zeng, H. Zhang, H. Zhao and W. Liu, *Int. J. Electrochem. Sci.*, 7 (2012) 11264.
25. S.-B. Lee, S.-I. Pyun and E.-J. Lee, *Electrochim. Acta*, 47 (2001) 855.
26. D. Carmier, C. Vix-Guterl, J. Lahaye, *Carbon* 39 (2001) 2181.
27. P. G. Russell, F. Goebel, *J. Power Sources*, 54 (1995) 180.